Possible improvements of the method of fundamental solution to solve the ECGI problem

Judit Chamorro-Servent, Laura Bear, Josselin Duchateau, Mark Potse, Rémi Dubois, Yves Coudière

Possible improvements of the method of fundamental solution to solve the ECGI problem

Judit Chamorro-Servent[1,2,3], Laura Bear[1,4,5], Josselin Duchateau[1,4,5], Mark Potse[1,2,3], Rémi Dubois[1,4,5], Yves Coudière[1,2,3]

[1]IHU Liryc, Electrophysiology and Heart Modeling Institute, foundation Bordeaux Université, F-33600 Pessac-Bordeaux, France
[2]CARMEN Research Team, INRIA, F-33400 Talence, France, [3]Univ. Bordeaux, IMB, UMR 5251, CNRS, INP-Bordeaux, F-33400 Talence, France,
[4]Univ. Bordeaux, Centre de recherche Cardio-Thoracique de Bordeaux, U1045, F-33300 Bordeaux, France, [5]INSERM, Centre de recherche Cardio-Thoracique de Bordeaux, U1045, F-33300 Bordeaux, France

Introduction

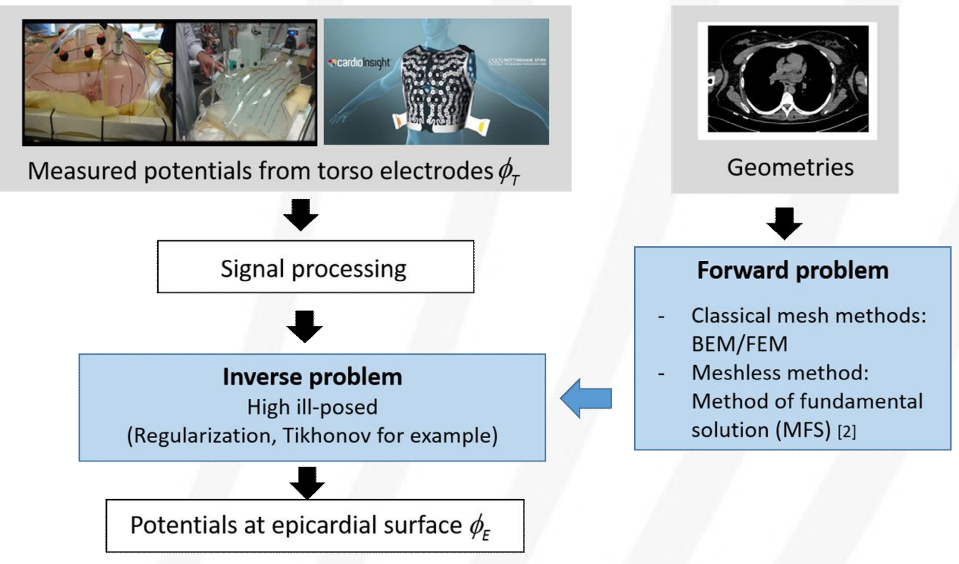

➢ Despite all the success of ECGI, the understanding and treatment of many cardiac diseases is not feasible yet without an improvement of the inverse problem solution.

➢ ***Can we improve the forward problem to make the inverse problem less ill-conditioned?***

➢ Robust calculations of the inverse ECGI problem may require accurate specification of **boundary conditions** at the torso and cardiac surfaces [1].

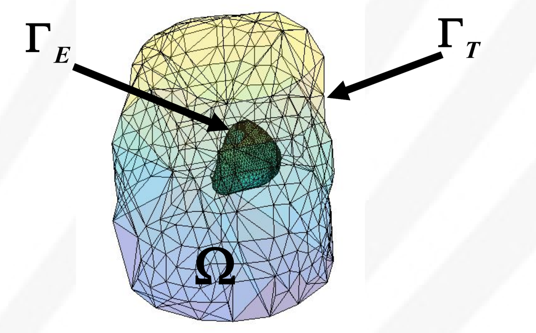

Geometrical meshes used: The body is cut at the top and bottom of the torso and the arms.

$-div(\phi)$,in Ω. Under: (1)

Dirichlet conditions: $\phi=\phi_T$ on Γ_T

Homogeneous Neumann conditions: $\partial_n\phi=0$ on Γ_T

The aim of the inverse problem is to find $\phi=\phi_E$ on Γ_E

➢ The classical formulation of the ECGI inverse problem with the method of fundamental solution (MFS) involves a linear system [2].

Study of Boundary conditions

➢ The MFS matrix can be split in two matrices:

$$
\begin{array}{c}
\text{Dirichlet Conditions } B_0 \\
\\
\text{Homogeneous Neumann Conditions (HNC) } B_1
\end{array}
\begin{pmatrix}
1 & f(\|x_1-y_1\|) & \cdots & f(\|x_1-y_M\|) \\
\vdots & & \cdots & \vdots \\
1 & f(\|x_N-y_1\|) & \cdots & f(\|x_N-y_M\|) \\
0 & \frac{\partial f(\|x_1-y_1\|)}{\partial n} & \cdots & \frac{\partial f(\|x_1-y_M\|)}{\partial n} \\
\vdots & & \cdots & \vdots \\
0 & \frac{\partial f(\|x_N-y_1\|)}{\partial n} & \cdots & \frac{\partial f(\|x_N-y_M\|)}{\partial n}
\end{pmatrix}
*
\begin{pmatrix} a_0 \\ a_1 \\ \vdots \\ a_M \end{pmatrix}
=
\begin{pmatrix} \phi_T(x_1) \\ \vdots \\ \phi_T(x_N) \\ 0 \\ \vdots \\ 0 \end{pmatrix}
$$

$$x_i \in \Gamma_T, y_j \in \hat{\Gamma}_T \cup \hat{\Gamma}_E$$

$$f(\|x_i-y_j\|)=\frac{1}{4\pi\|x_i-y_j\|}$$

$$\phi_E(x)=a_0+\sum_{j=1}^{M}a_j f(\|x-y_j\|),$$

$$x \in \Gamma_E, y_j \in \hat{\Gamma}_T \cup \hat{\Gamma}_E$$

➢ We can remark that:
- The contribution of the submatrices B_1 and B_0 in the whole solution is related to their respectives norms.
- Due to the meshing of the torso, non-physiological conditions are applied to the top, bottom of the torso and the arms.
- Accurate computation of the normals at torso surface is required.

Do we need to enforce the homogeneous Neumann conditions in the MFS inverse problem?

•To evaluate the contribution of both **boundary conditions**:

$$J_\lambda(a)=\frac{1}{2}\left((1-\lambda)^2\|B_0a-\phi_T\|_2^2+\lambda\|B_1a\|_2^2+\alpha\|a\|_2^2\right), \text{ for } \lambda=0 \text{ (MFS without HNC) and } \lambda=0.5 \text{ (Standard MFS)} \quad (4)$$

The solution of (4) was found by using Tikhonov regularization and α was chosen by using Creso method as in [2].

Study of placement of virtual sources

➢ In other fields it has been shown that the ill-posedness of MFS problem and the efficacy of its solution depends on **the placement of the virtual sources** [3].

➢ The center of the heart used in [2] to inflate the torso surface (in order to place its respective virtual sources) can be a misfit reference, for example when structural diseases are present.

➢ Therefore, we studied **the effect of changing the torso virtual placement**:

i. For each electrode on the torso, we find the location of closest point on the heart surface $h_{d_{\min}}$ s.t. $d_{\min}=\min\left(\|x_i-h_k\|_2\right), k=1,\cdots,M_H$

ii. We construct the location of virtual source y_i related to the torso electrode x_i as $y_i=x_i+R_T\left(x_i-h_{d_{\min}}\right)$

iii. We use SVA to find the ratio R_T that makes our problem better Conditioned, i.e. that improves the SV decay.

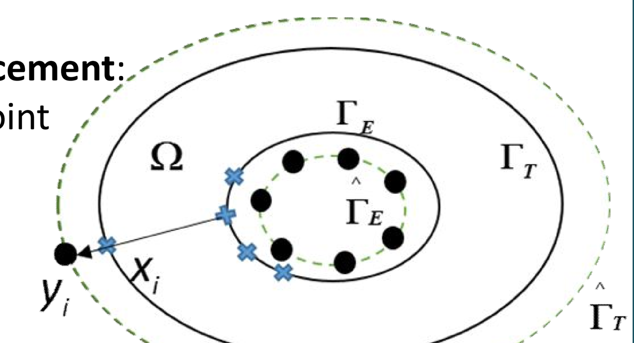

Method of evaluation

➢ *To test the effect of HNC* – **Five activation patterns** (1 single site pacing and 4 single spiral waves) **were simulated** using [4]:

i. The currents from the monodomain problem are used to compute the BSPM. The simulations provide both the theoretical, *in-silico* ϕ_T and ϕ_E every 1ms.

ii. ϕ_T were computed by solving a static bidomain problem in a realistic, heterogeneous torso model.

➢ *To test the ill-posedness of the problem* with standard and new *distribution of sources* – **Real data** from a patient presenting scar was employed.

➢ To compare the four combinations: Standard MFS, Standard MFS without HNC, MFS with new distribution of sources, and MFS with new distribution of sources and without HNC – **Experimental data** (LBBB) from:

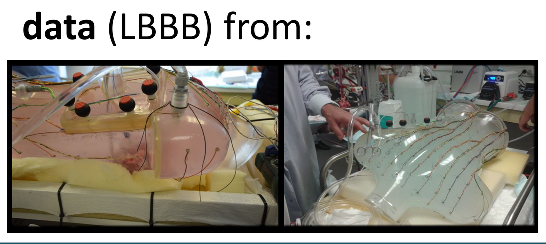

256 electrodes at torso(128 obtained)
Sinus rhythm pacing
for epi /endo surfaces

108 electrodes at sock

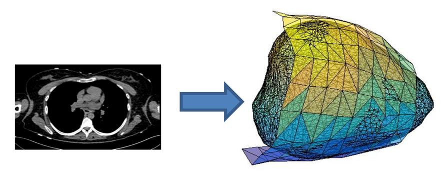

Heart and sock meshes

Results

➢ **Study of Boundary conditions: Respective contribution of B0 and B1**

- The $\varepsilon=\|B_1\|/\|B_0\|$ depends only on the geometry and location of sources (for which we used a fixed rule defined in [2]). We found $\varepsilon=0.0013$, indicating predominance of B_0 compared to B_1 in the standard MFS.

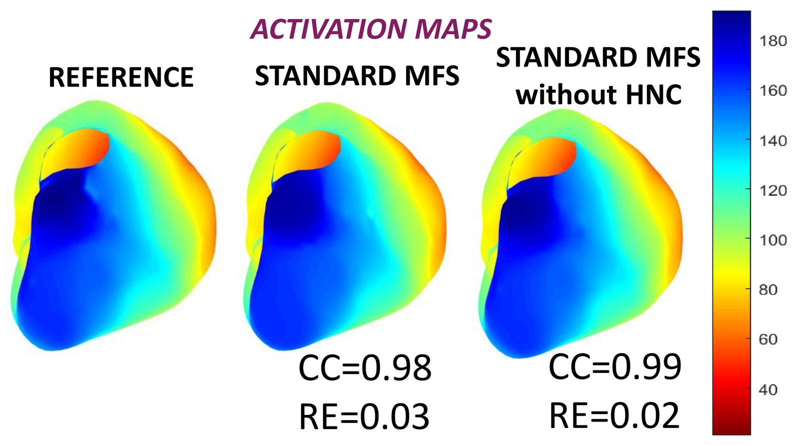

Figure 1. Activation maps for electrograms, single site pacing.

COMPARISON OF ELECTROGRAMS						
	CC			RE		
	Q_1	Median	Q_3	Q_1	Median	Q_3
STANDARD MFS	0,999	0,999	0,999	0,020	0,034	0,054
STANDARD MFS without HNC	0,989	0,995	0,998	0,071	0,107	0,152

Table 1. CC and RE for electrograms, five simulations.

➢ **Study of the effect of changing the torso virtual sources placement**

- The new distribution of torso virtual sources reduces the ill-posedness of the problem

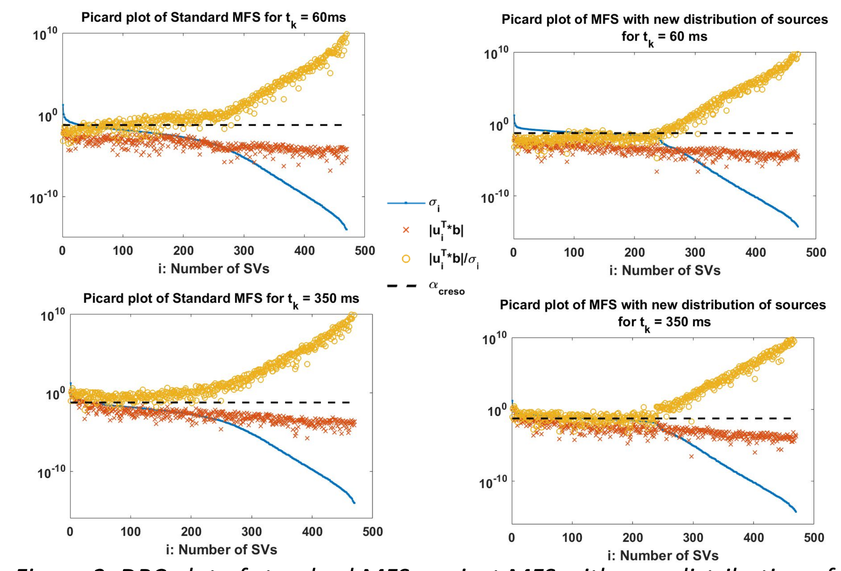

Figure 2. DPC plot of standard MFS against MFS with new distribution of sources for two instances of time different. (Data from patient with scar)

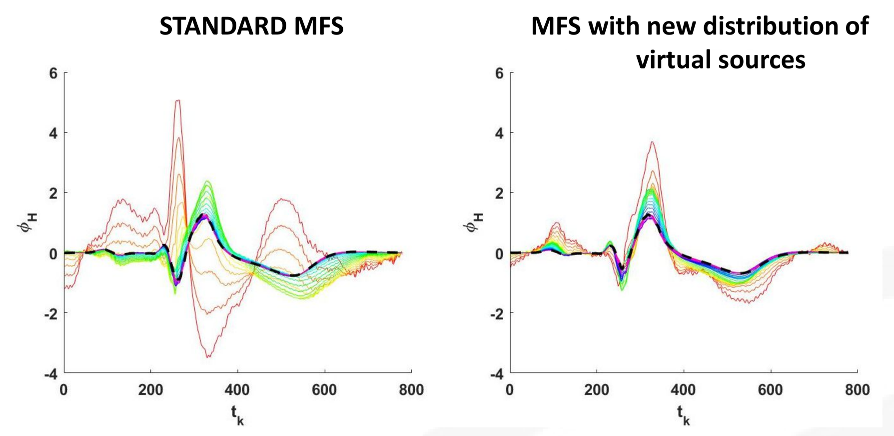

Figure 3. Reconstructed potentials for different parameters of regularization. (Data from patient with scar)

➢ **Combining the effect of changing the placement of virtual sources in the torso with the effect of HNC**

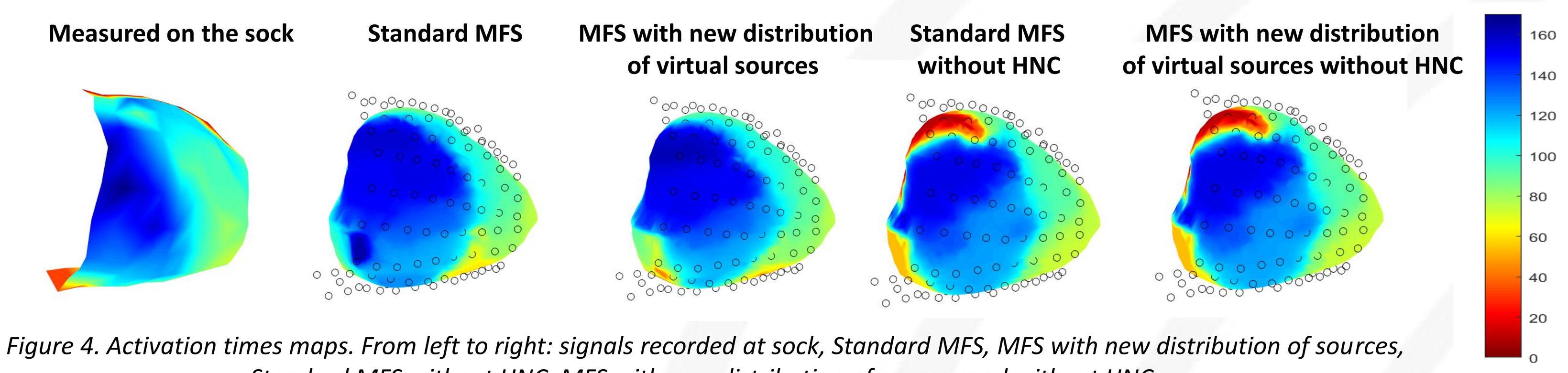

Figure 4. Activation times maps. From left to right: signals recorded at sock, Standard MFS, MFS with new distribution of sources, Standard MFS without HNC, MFS with new distribution of sources and without HNC.

COMPARISON OF ATs		
	CC	RE
STANDARD MFS	0,57	0,37
STANDARD MFS, NO HNC	0,66	0,34
MFS with NEW DIST.	0,61	0,35
MFS with NEW DIST., NO HNC	0,58	0,38

Table 2. CCs and REs for Ats maps above (figure 4).

COMPARISON OF ELECTROGRAMS						
	CC			RE		
	Q1	Median	Q3	Q1	Median	Q3
STANDARD MFS	0,32	0,41	0,68	0,54	0,78	1,03
STANDARD MFS, NO HNC	0,28	0,5	0,77	0,57	0,75	0,96
MFS with NEW DIST.	0,24	0,49	0,75	0,58	0,74	0,95
MFS with NEW DIST., NO HNC	0,29	0,55	0,78	0,38	0,61	0,61

Table 3. CCs in the interval (beat) outlined by the orange box and REs for potentials below (figure 5).

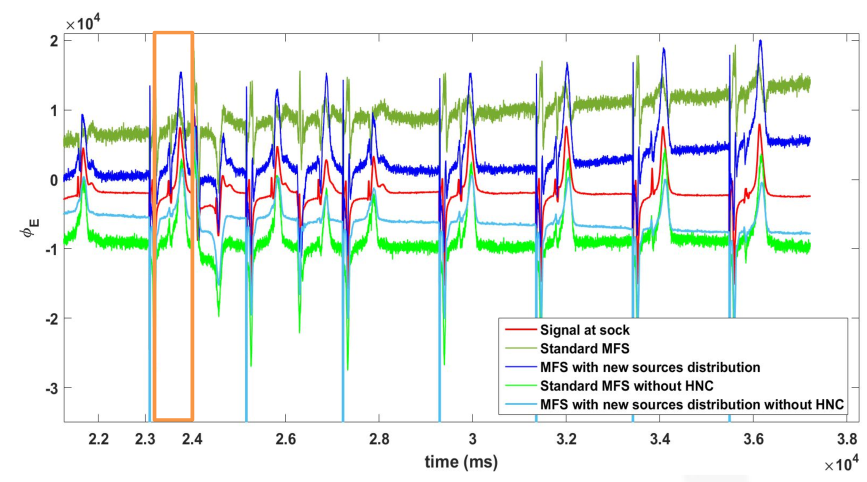

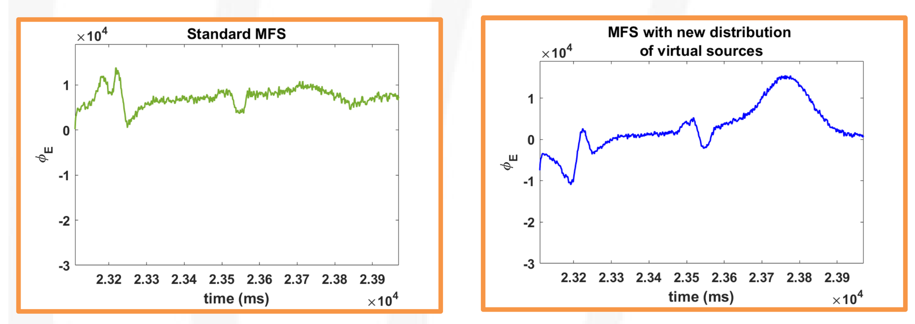

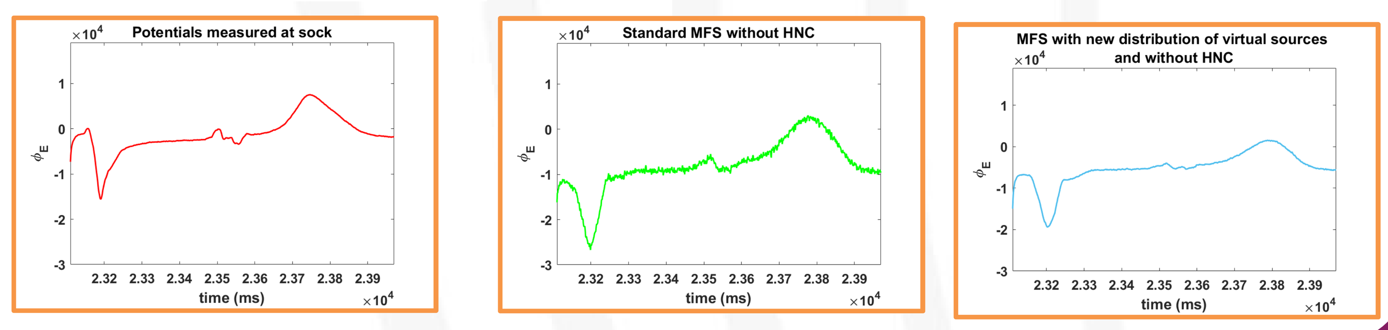

Figure 5. Potentials reconstructed by the 4 combination of methods against potentials recorded on the sock.

Conclusions

➢ Removing the Neumann conditions reduces the forward and inverse computational cost.

➢ MFS with new distribution of sources made the problem less ill-conditioned and less sensitive to the choice of the regularization parameter.

➢ The HNC are related with the small SVs, i.e. with higher frequencies, this can be seen in the respective noisy reconstructed potentials.

➢ MFS with new distribution of virtual sources and without HNC has better CC and less REs. However, the REs are still high. This indicates that a good similarity of the potential pattern is achieved but not a good amplitude. Finally, best ATs maps were achieved by standard MFS without HNC.

➢ Future work: The amplitude can be improved with better choice of the regularization parameter according to the distance of the virtual sources and/or by using spatio-temporal regularization.

Acknowledgements

This study received financial support from the French Government as part of the « Investissement d'avenir » program managed by the National Research Agency (ANR), Grant reference ANR-10-IAHU-04 from the Conseil Régional Aquitaine as part of the project « Assimilation de données en cancérologie et cardiologie ».

References

[1] Barr R, et al. Relating epicardial to body surface potential distributions by means of transfer coefficients based on geometry measurements. *IEEE Trans Biomed Eng Jan* 1977; BME-24 (1): 1-11.
[2] Wang Y, Rudy Y. Application of the method of fundamental solutions to potential-based inverse electrocardiography. *Annals of Biomedical Engineering* Aug 2006; 34(8): 1272-1288.
[3] Karageorghis A, et al. A survey of applications of the MFS to inverse problems. *Inverse problems in science and Engineering* 2011; 19(3): 309-336.
[4] Potse M, et al. Cardiac anisotropy in boundary-element models for the electrocardiogram. *Medical & Biological Engineering & Computing*. 2009, 47(7): 719-729.